Multi-wavelength Raman lidar observations of the Eyjafjallajökull volcanic cloud over Potenza, Southern Italy

L. Mona, A. Amodeo, G. D'Amico, A. Giunta, F. Madonna, G. Pappalardo
{Consiglio Nazionale delle Ricerche – Istituto di Metodologie per l'Analisi Ambientale (CNR-IMAA), C.da S. Loja, I-85050 Tito Scalo, Potenza, Italy }
Correspondence to: L. Mona (mona@imaa.cnr.it)

Abstract

Multi-wavelength Raman lidar measurements were performed at CNR-IMAA Atmospheric Observatory (CIAO) during the entire Eyjafjallajökull explosive eruptive period in April-May 2010, whenever weather conditions permitted.

A methodology for volcanic layer identification and accurate aerosol typing from the multi-wavelength Raman lidar measurements has been developed taking advantage from the long-term lidar measurements performed at CIAO since 2000. The aerosol mask for lidar measurements performed at CIAO during the 2010 Eyjafjallajökull eruption has been obtained. Volcanic aerosol layers have been observed in different periods: 19-22 April, 27-29 April, 8-9 May, 13-14 May and 18-19 May. A maximum aerosol optical depth of about 0.12-0.13 was observed on 20 April, 22:00 UTC and 13 May, 20:30 UTC. Volcanic particles have been detected both at low altitudes, in the free troposphere and in the upper troposphere. Intrusions into the PBL have been revealed on 21-22 April and 13 May. For the period under investigations, a Saharan dust intrusion was observed on 13-14 May: dust and volcanic particles have been simultaneously **detected** at CIAO both at separated different levels and mixed within the same layer.

Lidar ratios at 355 and 532 nm, Ångström exponent at 355/532 nm, backscatter related Ångström exponent at 532/1064 nm and particle linear depolarization ratio at 532 nm measured inside the detected volcanic layers **are** discussed. The dependence of these quantities on relative humidity has been investigated by using co-located microwave profiler measurements. **The study of these intensive parameters indicate the presence of volcanic sulfates/continental mixed aerosol in the volcanic aerosol layers observed at CIAO. Differences observed in correspondence of the two maxima in the volcanic aerosol load indicate the presence, besides sulfates aerosols, of some aged ash.**

1 Introduction

On 14 April 2010 Eyjafjallajökull, **a small volcano under Iceland's ice cap**, entered an explosive eruptive phase after an effusive eruptive period started in March 2010. **This medium-sized eruption (Petersen, 2010) caused an enormous disruption to air traffic across western and northern Europe, because it injected ash directly into the Jet Stream and from there in the northern Europe free troposphere.** The explosive eruptive period lasted until 21 May 2010, with variable intensity, emission of material and plume height (Langmann et al., 2011).

Since the first explosive eruption of Eyjafjallajökull volcano on 14 April 2010, aerosol scientific community has largely been focused on the monitoring and study of the volcanic cloud. EARLINET, the European Aerosol Research Lidar NETwork, has performed almost continuous measurements since 15 April 2010 in order to follow up the evolution of the volcanic cloud generated from the eruption of the Eyjafjallajökull volcano. EARLINET measurements **were** performed **according** to alerts distributed by CNR-IMAA based on the model calculations of the ash dispersion provided by the VAAC (Volcanic Ash Advisory Center) and EURAD (EURopean Air Pollution Dispersion). **Almost the whole European continent was affected by the arrival of the volcanic cloud. Volcanic particles were observed in UK, Germany and France from very low altitude up to the upper troposphere for almost the whole 2010 Eyjafjallajökull eruptive period (Pappalardo et al., 2010a; Emeis et al., 2011; Flentje et al., 2010; Schumann et al., 2011). The cloud reached Italy and Greece starting from 19-20 April, after passing the Alps (Pappalardo et al., 2010a). In May 2010, the volcanic cloud was transported over the Iberian Peninsula moving then towards East, reaching again Italy and Greece (Pappalardo et al., 2010a).** First studies concerning the large amount of volcanic particles observed over Central Europe during the volcanic event based on remote sensing observations have already been published in the peer-reviewed literature (Ansmann et al., 2010; Flentje et al., 2010; Emeis et al., **2011**; Gasteiger et al., **2011**; Schumann et al., 2011). Nowadays, there is still a lack of information related to the Eyjafjallajökull plume observations in Southern Europe. Anyway, the arrival of the volcanic cloud in the Mediterranean region is particularly interesting for several reasons. **Firstly, the large distance from the volcano and the low amount of aerosols reaching this area make the observations of the volcanic cloud in Mediterranean region useful and necessary for the evaluation of different models (e.g.**

Matthias et al., 2011; Stohl et al., 2011) at the extremes of their operability, i.e. for low aerosol concentration and at far distances from the emitting source. Secondly, the observations at locations far away from the source allow us to investigate any modification in aerosol properties occurred during the transport as well as mixing processes across the European continent. In addition, Saharan dust intrusions in Southern Europe are typical in Spring and Summer thus offering an opportunity to study the differences and mixing of volcanic aerosols with desert dust particles. Finally, it is worth considering that since the Mediterranean is an almost closed basin, the volcanic plume arrived, even if less intense than in Central and Northern Europe, could affect the Mediterranean ecosystem.

In this paper, we are presenting and discussing the observations concerning the Eyjafjallajökull volcanic particles performed at CNR-IMAA, Potenza, Southern Italy (40°36'N, 15°44'E, 760 m above sea level).

CNR-IMAA is an EARLINET core station due to its long-term observations (it has been participating in the network since its beginning in 2000) and its **state-of-the-art** multi-wavelength Raman lidars. Moreover, the CNR-IMAA runs an advanced observatory, named CIAO (CNR-IMAA Atmospheric Observatory), equipped with the state-of-the-art instruments for the **ground based** remote sensing of aerosol, water vapour and clouds (Madonna et al., 2010a). Finally, the first Raman lidar measurements of volcanic aerosol in troposphere were performed during the 2002 Etna volcanic eruption right at CNR-IMAA (Pappalardo et al., 2004a) and these observations were object of a detailed study based on an integrated approach between lidar observations and transport modeling (Villani et al., 2006). Taking advantage both of this expertise and the long-term database of lidar observations collected at CIAO, a methodology for identifying the volcanic aerosol layer in the aerosol vertical profile time-series has been developed. **Indeed, it is well know that lidar measurements are particularly effective for the near real time identification of high aerosol content. However, reliable and quantitative layering identification, clouds screening and aerosol typing are still critical issues. There are different automated methods, such as that used for the CALIPSO retrievals (Liu et al., 2010), which aim to provide reliable results in near-real time. This kind of algorithms relies on the idea that the whole range of possibilities in terms of optical properties have already been measured and characterized for each aerosol class. Therefore, these algorithms are not feasible for particular scenarios such as tropospheric volcanic clouds because of both the specificity of each volcanic eruption in terms of emitted particles and the overall scarcity**

of observations related to this kind of events. In contrast, the multi-wavelength Raman lidar has been widely demonstrated to be an effective tool for the aerosol characterization and for the investigation of modification processes occurred during the transport and the mixing of aerosol types (e.g. Müller et al., 2007; Papayannis et al., 2008). Moreover, it has been shown that a careful analysis based on lidar observations, air-mass backtrajectories and modeling tools is needed for a detailed classification of the observed aerosols (e.g. Mona et al., 2006b, Müller et al., 2009; Villani et al., 2006, Pappalardo et al., 2010c).

After a short description of lidar measurements performed at CIAO during the Eyjafjallajökull eruptive period, the developed methodology for aerosol masking is described in Section 3. The aerosol masks for the observations collected during the 15 April – 20 May 2010 period are reported in Section 4 which also reports results in terms of the aerosol optical properties of the identified volcanic aerosol layers. Finally, a summary is given.

2 Lidar measurements

The current study mainly relies on lidar measurements performed by PEARL (Potenza EArlinet Raman Lidar), the multi-wavelength lidar system for tropospheric aerosol characterization designed and operated by CNR-IMAA since August 2005 (Mona et al., 2009). This system is an upgrade of a pre-existing Raman lidar system for tropospheric aerosol **studies** which has been operative since the EARLINET beginning in 2000 (Mona et al., 2006b). PEARL measures the radiation elastically backscattered from the atmosphere at three laser wavelengths (355 nm, 532 nm and 1064 nm), the N_2-Raman shifted radiation backscattered at 387 nm and 607 nm, and the perpendicular and the parallel polarized components of the 532 nm backscattered light (with respect to the linearly polarized laser beam direction). Simultaneous aerosol extinction and backscatter profiles at 355 and 532 nm are retrieved with the combined elastic-Raman retrieval (Ansmann et al., 1992). **This allows us to measure directly the lidar ratio (extinction to backscatter ratio) vertical profile both at 355 and 532 nm. Additionally, the aerosol backscatter at 1064 nm is retrieved through an iterative procedure (Di Girolamo et al., 1999), with a lidar ratio profile selected on the basis of the lidar ratio profiles measured at 355 and 532 nm. Summarizing, aerosol backscatter coefficient profiles at 3 wavelengths (355, 532 and 1064 nm) and extinction profiles at 2 wavelengths (355 and 532 nm) are simultaneously**

measured at CIAO. This ensemble of measurements will be referred as 3+2 measurements in the following. The particle linear depolarization ratio profile at 532 nm is retrieved by using the "0°-calibration" technique as described in Freudenthaler et al., 2009. More technical details of **the PEARL set-up and the retrieved products** can be found in Madonna et al., 2010a and Mona et al., 2009.

In order to meet both scientific and public interests in this volcanic eruption, lidar measurements were performed at CIAO during the alert periods, whenever weather conditions permitted, accordingly to EARLINET observational strategy established for this volcanic eruption event (Pappalardo et al., 2010b). There were two main periods of volcanic-cloud transport over Europe (Pappalardo et al., 2010a): 15-30 April, when wind transported the emitted material over Central Europe and then towards the South-Southeast; after 5 May, when most of the Eyjafjallajökull volcano emissions reached almost directly Western Europe and then were transported towards Italy, Greece and the Balkans.

From 15 April, when the first alert was sent, lidar measurements were performed at CIAO whenever the absence of low clouds and rain permits them. During 19-22 April period the arrival of volcanic ash over Northern and Central Europe and, after that, a feeble transport of ash beyond the Alps were forecast. In 25-30 April period, desert dust arrived over Southern Europe followed by a change in the wind direction with air masses coming from North-Eastern Europe, potentially transporting material emitted by the Eyjafjallajökull volcano over Western Europe and then over Italy and Greece. This situation lasted for the following days, when Saharan dust intrusions over Southern Europe also occurred. A possible arrival of volcanic cloud over Northern Italy was forecast for 8 May. Accordingly, lidar measurements were performed from 8 May, 20:00 UTC till 11 May, 02:00 UTC. CIAO ran lidar measurements from 12 May, 12:00 UTC, till 15 May, 01:00 UTC, when a shower forced a sudden stop. The last measurements performed for the Eyjafjallajökull volcano eruption started on 18 May, 06:00 UTC, and continued until 19 May, 11:00 UTC.

Quick-looks of time series of elastically backscattered lidar signals were made available in near real time at CNR-IMAA web site (www.imaa.cnr.it) in order to satisfy national and international requests for information on the volcanic cloud detection for both scientific and public aims. A link to an EARLINET quick-look web-page (www.earlinet.org) allowed an easy and fast overview of the aerosol layers over Europe during the whole period. In addition, a daily report of CIAO volcanic cloud observations was delivered and collected together with those of the other EARLINET stations summarizing relevant information on volcanic cloud over Europe. Regarding CIAO observations, a preliminary quick analysis showed 4 periods that could be affected by the arrival of volcanic particles: 19-22 April, 27-29 April, 8-10 May, 12-14 May and 18-19 May.

3 Methodology

A big effort was made at CIAO to collect as large database as possible of volcanic-related lidar observations. Periods probably affected by the arrival of emitted volcanic materials over Italy were identified by a preliminary near-real time inspection of these data. However, the aim of this paper is to describe the temporal and vertical evolution of the volcanic aerosol content over a lidar station located far away from the volcano, where the amount of volcanic aerosol is much lower than that observed in Central Europe (e.g. Schumann et al., 2011, Ansmann et al., 2010; Gasteiger et al., 2010), and in a period in which Saharan dust intrusions are often observed in Southern Europe. Therefore, a detailed and specific analysis is needed to investigate the time and range resolved occurrences of volcanic cloud observations.

An appropriate methodology has been developed by following a step procedure consisting of: i**)** the identification of particle layers; ii) cloud vs aerosol discrimination iii) aerosol typing through the investigation of intensive properties measured by multi-wavelength Raman lidar and models and back-trajectory analysis.

This methodology permits to obtain a quantitative and reliable aerosol masking starting from lidar measurements going beyond the precious but still qualitative layering information provided by the temporal evolution of the range corrected lidar signal provided in near-real-time during the volcanic event. As example Figure 1 reports the temporal evolution of the range corrected lidar signal measured at 1064 nm at CIAO in the 12 -14 May period. From this figure, it is clear the effectiveness of lidar measurements in the atmospheric layering. The signature of a strong particle layer about 1-1.5 km deep is evident at the beginning of the measurement record decreasing in altitude from 5 to 3 km a.s.l.. In the early morning of 13 May, the arrival of a **tenuous** layer is distinguishable at 6 km, **descending** in the following hours and becoming **a dense** but very thin layer located around 2-2.5 km from the evening of 13 May until the early morning of 14 May. Frequent and short intense lidar returns are evident below 2 km between 13 May, 12:00 UTC, and 14 May, 04:00 UTC, when measurements were interrupted because of low clouds and light rain. Aerosol layers were present up to 6 km on 14 May from 09:00 UTC to 23:00 UTC, when low clouds followed by intense rain forced the measurement stop.

3.1 Layers identification

An algorithm has been implemented for the quantitative identification of layers above the PBL. The main concept is that features can be identified through the first derivative of the particle backscatter profile. Other methods are reported in literature (e.g. Steyn et al., 1999; Wang and Sassen, 2008) where their enhanced capability in different conditions is shown. However, the results obtained by using all these methods agree within the experimental errors. **With respect** to commonly used procedures for aerosol/cloud identification (e.g. Morille et al., 2007; Vaughan et al., 2004), the advantage of our approach is that of starting from calibrated backscatter profiles, whose high quality is certified by the EARLINET quality assurance program (Böckmann et al., 2004; Pappalardo et al., 2004), rather than from quasi raw signals (namely the range corrected signals). This makes it possible to overcome problems related to the normalization processes applied in automated methods based on range corrected signals.

However, since the derivative is strongly sensitive to fluctuations, a smoothing procedure is typically needed. A second-order Savitsky-Golay filter is applied on the differential, because of its effectiveness in preserving vertical structures (Pappalardo et al., 2004b). The number of points is progressively increased as the signal noise increases, with 1000 m as fixed maximum of the effective vertical resolution (Pappalardo et al., 2004b).

This method for the identification of layers can be applied only in regions where the relative statistical error on backscatter profile is sufficiently low. Tests performed on several EARLINET station data have made it possible to identify 30% as a reasonable limit for the application of the derivative method. In the altitude region characterized by a relative error on aerosol backscatter coefficient higher than 30%, layers are identified as those regions where **the scattering ratio (i.e. the total to molecular backscatter ratio)** is higher than a pre-defined threshold. **In particular, particle layers should correspond to a scattering ratio significantly higher than the value observed for aerosol background condition. The scattering ratio background value is evaluated on the basis of the long-term aerosol observations performed at CIAO since 2000, in the 6.5-8.5 km altitude range, typically not affected by an intense particle transport.** Particle layers are identified as altitude regions where the scattering ratio is higher than the defined threshold plus the scattering ratio absolute statistical error.

The layer identification is performed above the PBL top altitude calculated by using the procedure established within EARLINET (Matthias et al., 2004). In this way, layers consisting of transported aerosols (like Saharan dust and volcanic aerosol) can be identified. Regarding the PBL region, intrusions from upper level layers would lead to a mixing of local aerosol (typically confined in the PBL) with transported aerosol. These situations will be identified on the basis of the temporal evolution of the layers and modification of aerosol optical properties in the PBL region.

Finally, only the altitude ranges where the statistical error on backscatter coefficient is lower than 50% are considered in this spatio-temporal evolution study, for providing only reliable information on the aerosol masking.

A compromise between the high temporal resolution available for the backscatter profiles and a longer time average, needed to reduce the statistical error, is necessary. **A temporal average of 1 hour is chosen in order to be able to draw a direct comparison with models that typically provide data every hour (e.g. Matthias et al., 2011).**

The aerosol backscatter coefficient at 1064 nm is used for the layering taking advantage of the stronger sensitivity to the aerosol structures at this wavelength **with respect** to visible and ultraviolet ones. The effective vertical resolution is chosen each time as the best possible to optimize relative error and vertical profiling capability, and it is typically 60 m for the cases under investigation. The routine for the particle layer identification runs on individual backscatter profile. As final step, a consistency check is performed on the resulting layering temporal evolution.

Figure 2 reports an example of single profile particle layer identification, as performed on the aerosol backscatter profile at 1064 nm measured on 13 May, at 05:30-06:30 UTC. The base and top of each layer are indicated as dotted and solid horizontal lines, respectively. A detailed layering structure characterization is obtained up to the upper troposphere, indicating the presence of an aerosol load higher than what is typically measured at CIAO up to 12 km a.s.l.. The derivative technique (applied below the 30% error limit, i.e. black region in the plot) allows us to characterize the internal structure of multi-stratified complex aerosol layers, identifying 5 distinct aerosol layers above the PBL top up to **7** km altitude region on the basis of the aerosol backscatter gradient analysis. **At upper levels, the applied**

methodology allows the identification of thin and sparse layers as exceeding the threshold on the scattering ratio. This is an indication of the presence of a low amount of aerosol at these altitudes. The further check of the temporal evolution of the layers indicates that these signatures are present not only at this time but also at the following ones. All these elements allow for an objective identification of these features as aerosol layers distinguishable from the measured backscatter profiles. At altitude higher than 12 km a.s.l., longer integration time, or a time series analysis, could allow us to better describe the upper level particle layers.

3.2 Clouds identification

After the identification of the particle layers, the type of the observed particles has to be identified. A first preliminary discrimination is carried out between aerosol and clouds. **Cirrus clouds are identified mainly on the basis both of their temporal dynamical evolution (Mona et al., 2007), the high particle linear depolarization ratio and the almost neutral backscatter spectral dependence, due to the large size of hydrometeors.** Following EARLINET protocol, low clouds are removed from the backscatter profile evaluation by the eye-inspections of single raw data. The analysis of the temporal evolution of the retrieved aerosol backscatter profile is an additional check of the appropriateness of low cloud removing procedure.

3.3 Aerosol typing

Backward trajectory analyses and model outputs are used to investigate the origin and the nature of the aerosol layers identified through the procedure described in 3.1. In particular, 10-day HYSPLIT backtrajectory analysis provided by NOAA (Draxler, R.R. and Rolph, G.D., 2011) is used because of its larger flexibility. Actually, 3 arrival altitudes can be set by the users on the basis of specific needs, and the arrival time can be chosen with a 1-hour resolution. These options make the HYSPLIT backtrajectory analysis very flexible for the aerosol typing in an integrated study with high vertical and temporal resolution lidar data. The use of backtrajectory analysis for the identification of aerosol origin is nowadays well recognized, especially for large source areas such as desert regions. Deeper attention should be paid in the presence of an almost punctual source, as in the case of volcanic eruptions and in particular for observations performed at long distances from the source, because the particle position uncertainty increases with the trajectory length, with lower uncertainty for higher wind speed (Stohl, 1998). For potential volcanic eruption cases, the stability of the aerosol typing is checked by slightly changing both arrival altitudes and times. In addition, other backtrajectory analyses are used as further checks: 4-day backward trajectories provided by the German Weather Service (DWD) at each EARLINET lidar station for two arrival times per day and for six arrival pressure levels between 200 and 975 hPa (Stohl, 1998); FLEXTRA trajectory model (Stohl et al., 1995) provided for each EARLINET site every 6 hours at 1500, 3000 and 5000 m as arrival altitudes; and Trajectory Analysis developed by the Atmospheric Chemistry and Dynamics Branch of the NASA/Goddard available for each AERONET site at 00:00 UTC and 12:00 UTC for 8 height levels between 950 and 200 hPa (Schoeberl and Newman, 1995).

Once the particle path is identified, the occurrences of a specific event along the path is checked against both related models and satellite data, when available, **for the identification of** the potential aerosol source (for example desert, volcano and fires). In particular, DREAM (Dust REgional Atmospheric Model) forecasts are used for Saharan dust in terms of maps of the dust loading over the Mediterranean and dust concentration profiles over Potenza EARLINET site, both available every 6 hours. The Eyjafjallajökull volcanic activity and emission heights are checked through updated reports provided by the Iceland Meteorological Office, VAAC and EURAD forecasts and dedicated studies (e.g. Langmann et al 2011). Finally, the presence of forest fire episodes is checked by using the World Fire Atlas available at http://wfaa-dat.esrin.esa.int/, based on ATSR Active Fire Algorithm.

Special attention must be paid to the transition between different atmospheric conditions and aerosol types arrivals. Indeed, there is high instability of the backtrajectory analysis in the transient regime among the different situations, which is also due to the uncertainties affecting the backtrajectory analysis. For such cases, small changes in time (profiles are obtained with 1 hour integration time) and/or in altitudes result in large differences in the air mass travelling path both in horizontal and vertical dimensions. In such cases, the identification of the aerosol layers through the analysis of one wavelength backscatter lidar (Sect. 3.2) and the combined use of models and backtrajectories is not sufficient, and would lead to an undefined aerosol zone in the resulting aerosol mask. In this context the single backscatter lidar technique is not sufficient to characterize aerosol and a reliable identification of the aerosol typing is possible only using multi-wavelength lidar measurements. Moreover, the long term lidar measurements performed at CIAO is an added value for the aerosol typing. In

particular, intensive properties and their temporal evolution are used here for discriminating different aerosol types, as dust and volcanic particles when uncertain situations occurred.

This uncertain situation occurred for example on 13 May around 05:00 UTC, during a transient between the presence of both dust and volcanic particles, but at separate levels, and the presence of only volcanic particles in a following time period.

The profiles of the aerosol backscatter at 1064 nm for this uncertain situation are reported in Fig. **3** together with the backscatter related Ångström exponent at 532/1064 nm. On 13 May, at 04:00 UTC, the backscatter related Ångström exponent at 532/1064 nm (in the following å(β)) has values ranging between 1.8 and 0.8 from the PBL top up to 4 km a.s.l., with a trend decreasing with the altitudes and a mean value of about 1 in agreement with the results obtained in a multi-year climatological study of Saharan dust intrusions over Potenza (Mona et al., 2006b). The same mean value is found for the 4-6 km altitude range, even if characterized by larger oscillations due to a higher statistical error. Therefore, the two identified layers extending between PBL and 6.4 km a.s.l. are classified as Saharan dust aerosol layers.

The å(β) profile for 05:00 UTC shows the same dependence on the altitude in the 2.1-3.2 km range with a shift toward lower values with respect to what is measured at 04:00 UTC. Between 3.2 and 6.4 km a.s.l. the aerosol backscatter profile is different from the previous one, with the presence of 2 layers extending between 3.2 -4.9 km a.s.l. and 5.1-6.4 km a.s.l.. **For these layers, the mean å(β) value is 0.2. The significant change in the Ångström exponent indicates the arrival of particles with different properties. According to the air mass backtrajectories these altitudes are likely affected by the arrival of volcanic cloud. This indicates a mixing between dust and volcanic particles.**

The å(β) profile measured at 06:00 UTC has, instead, a completely different altitude dependence: å(β) is almost constant (about 1) with the altitude, indicating a homogeneous layer in term of aerosol dimension up to 3.4 km a.s.l., and the corresponding backscatter profiles at 532 and 1064 nm (see Fig. 2) decrease with the altitude and without pronounced peaks, as typically happens in well mixed situations, indicating a mixing between PBL aerosol and desert dust particles. The feeble feature extending between 3.4 and 4.3 km a.s.l. is characterized by å(β) around 0.2, significantly lower than those observed in dust and in dust/local mixed aerosol, indicating the mixing with volcanic larger particles. At upper levels (up to 6.8 km), the backscatter related Ångström exponent shows different values typically close to zero, indicating, for this case, the presence of volcanic aerosol.

This example demonstrates how the multi-wavelength observational capability and the climatological analysis available at the observational site could allow to overcome difficulties in the aerosol typing.

4 Results

The methodology described in the previous section is applied to all the periods identified as potentially affected by the volcanic cloud: 19-22 April, 27-29 April, 08-09 May, 13-14 May and 18-19 May. The resulting mask for each of these periods is described in depth, and optical properties are discussed as well. Finally, an overview of the volcanic aerosol optical properties is provided in Sect. 4.2.

4.1 Aerosol Masks

The result of the aerosol masking is reported in Figs. **4 and 5**, where volcanic aerosol layers are reported in different shades of grey, according to the mean aerosol backscatter at 1064 nm. Desert dust layers are reported in orange, magenta ranges denote local-volcanic mixing cases, and pale orange and pink correspond to local-dust and dust-volcanic mixed aerosols. It is worth considering that the observed particles of volcanic origin may be affected by modification processes and mixing with path-encountered air masses during the long-range transport because of the large distance between the source (volcano) and the measuring point. Cases in which a further significant aerosol source is identified are classified as mixed aerosols. PBL aerosols and clouds and/or cirrus clouds are reported in yellow and cyan, respectively. As far as this is concerned it is worth mentioning that other different sources from volcano and Sahara desert, and correspondingly other aerosol types, are taken into account: forest fires and continental aerosol. **All possible mixings among these types of aerosol were taken into account.** If the origin identification of the layer observed should not be possible at this stage, aerosols would be classified as unknown (purple).

4.1.1 19-22 April 2010

The first arrival of volcanic particles at CIAO was recorded on 19 April 2010 at 20:00 UTC, when the **considered** models did not forecast any other possible source for the observed aerosol layers and the backtrajectories showed air masses coming from Iceland and reaching Potenza. In the period 19 April, 21:00 UTC – 20 April, 21:00 UTC, the retrieval of 1-hour backscatter profiles was inhibited because of low clouds. Volcanic particles were present over the whole investigated altitude range for the entire measurement period. In daytime conditions, a smaller altitude range was investigated in terms of aerosol typing **with respect** to nigh-time conditions because of the established limit of 50% on statistical error. A mixing with PBL entrapped aerosol was observed since 21 April, 01:00 UTC, causing an increase in the PBL top up to 2.8 km a.s.l. (i.e. 2 km above the ground), which is an unusual value for night-time observations (Mona et al., 2009). At 10:00 UTC, this 2 km-deep layer splits into two sharp layers, one from the ground up to PBL top at 1.5 km a.s.l., and the other above the PBL up to about 3 km a.s.l.. The low PBL top altitude observed at this time indicates that these mixed aerosols almost fall to the ground, in agreement with **Scanning Electron Microscopy** (SEM) analysis carried out on the PM2.5 samples collected at CIAO during the period under study (Lettino et al., 2011). At upper levels the arrival of volcanic particles was still continuing. Another intrusion into the PBL is observed at 14:00 UTC, 22 April, when the natural increasing in the PBL top due to the solar heating results in the mixing between PBL aerosol and volcanic aerosol located just above it.

A complete multi-wavelength analysis for the most significant time-windows is performed when cloud cover permits: 20 April, 21:00-23:05 UTC and 21 April, 19:06 UTC – 22 April, 03:09 UTC (see Table 1 for mean values calculated within identified layers). In addition, aerosol extinction and backscatter at 355 nm are available on 19 April, at 19:53-20:36 UTC, together with the aerosol backscatter at 1064 nm. For 19 April, when there was no alert for volcanic particle arrival over Potenza, measurements at 532 nm were not available. Finally, backscatter related Ångström exponent at 532/1064 nm is available from diurnal measurements performed on 21 April, at 11:30-12:30 UTC.

A lidar ratio at 355 nm of 54 sr is observed on the first volcanic cloud arrival, in agreement both with the values measured at our station for the close-by volcanic event during the 2002 Etna eruption (Pappalardo et al., 2004a) and the Central Europe EARLINET measurements of Eyjafjallajökull volcanic plume (Ansmann et al., 2010). The large standard deviation of this lidar ratio value could indicate that the identified layer is not so homogeneous in terms of aerosol microphysical properties and this could be ascribed both to a small component of volcanic particles **with respect** to the background ones and the long complex transport path (Villani et al., 2006; Mona et al., 2006a). On 20 April, the maximum peak in the aerosol backscatter at 1064 nm ($3x10^{-7}$ $m^{-1}sr^{-1}$) is observed around 22:00 UTC at about 3.5 km a.s.l.. At the same time, the maximum in aerosol optical depth occurred with a value of 0.13 at 355 nm. Lidar ratio values calculated within the identified layers (around 2.5 and 3.5 km a.s.l.) are around 40 sr and 50 sr at 355 nm and 532 nm, respectively. The Ångström exponent (available only for the lowest of the 2 layers) of 1.4 indicates particles which are on average smaller than those observed in Central Europe (Ansmann et al., 2010). Correspondingly, the mean particle linear depolarization ratio at 532 nm is around 20%, which is significantly lower than the values around 35% measured in Germany for this volcanic event (Ansmann et al., 2010). These differences with Leipzig lidar measurements can be due both to the longer transport path and a possible contamination with continental aerosols. It is interesting to underline the low variability of lidar ratio in this case, which could indicate a more defined and homogeneous situation in terms of microphysical properties.

During the 19-22 April period, an increase in the mean particle size is observed: the backscatter-related Ångström exponent at 532/1064 nm decreases from 1.8 recorded on 20 April evening, to 1.2 during the 21-22 April night, passing through 1.3 diurnal measurement during the 21 April. Correspondingly, also the Ångström exponent decreases from 1.4 down to 1.1. On the other hand, the particle linear depolarization ratio slightly increases from 15 % up to 25% in the 19-22 April period, indicating an increase in the particle mean asphericity.

During the 21-22 April night, lidar ratio values up to 80 sr at 355 and 532 nm are observed. These values are larger than those observed in the previous phase for volcanic particles, but are also significantly larger than 37 sr at 355 nm typically obtained at CIAO (Mona et al., 2006a). The high lidar ratio and decreased Ångström exponent might be due to the hygroscopicity of the volcanic particles. This hypothesis is supported by the relative humidity measured by the microwave radiometer operative at CIAO: in the volcanic aerosols layer, a relative humidity around 20% is measured on 20 April evening, while it is around 50% on 21 April. In addition, the volcanic layer observed at 1.6-3.4 km a.s.l. is the result of the splitting of the 2 km-deep PBL: the volcanic aerosol intruded into the PBL on 21 April, around 01:00 UTC, after that the 2 km-deep PBL separated into 2 well defined layers, one confined below 1.5 km and the other extended between 1.6 and 3.4 km a.s.l.. In the light of this, the 1.6-3.4 km volcanic layer observed is probably affected by modification of aerosol optical properties because of the mixing with local aerosols.

4.1.2 27-29 April 2010

This event is completely different from the previous one in terms of aerosol amount and transport mechanisms. **On 23-24 April, it was rained for almost all the day and on 25 April a strong dust event was observed.** The unknown aerosol classification is reported for the observation on 27 April. Backtrajectory analysis for 27 April morning does not show any clear origin of the air masses. The limited number of hours available for the analysis as well as the availability of only diurnal measurements for this day do not allow us to take advantage either of the study of the layer temporal/vertical evolution or the Raman and multi-wavelength capabilities. On 29 April evening, however, there is the clear evidence of volcanic particle arrival at CIAO in the entire free troposphere. For this case, a peak in the aerosol backscatter coefficient at 1064 nm of about $2.3x10^{-7}$ $m^{-1}sr^{-1}$ is observed around 22:00 UTC at about 2 km a.s.l.. The complete multi-wavelength analysis available for the lowest and most intense aerosol layer (2.7-3.4 km a.s.l.) indicates, also for this case, the presence of smaller and more absorbing particles than those observed in Northern Europe (Ansmann et al., 2010).

4.1.3 8-10 May 2010

Since 5 May, wind directions over Europe changed **with respect** to the previous days, transporting the volcanic cloud almost directly over the Iberian Peninsula and then towards Italy, Greece and the Balkans. Measurements at CIAO started on 8 May accordingly to the plume dispersion forecasts. The reported methodology allows us to identify volcanic aerosol layering up to 10 km a.s.l.. In particular, the most intense layer is close to the surface just above the PBL top, with a peak in the aerosol backscatter coefficient at 1064 nm of about $1x10^{-6}$ $m^{-1}sr^{-1}$ observed at about 2 km a.s.l. at 18:00-22:00 UTC. Both particle linear depolarization ratio and Ångström exponents indicate the presence of particles on average larger and less depolarizing than those observed starting from 22 April night, but with similar lidar ratio values.

4.1.4 13-14 May 2010

The scenario observed during this period is characterized by a high variability with the presence of both wide and thin intense aerosol layers, cirrus, and sparse low clouds. Three main situations are observed on the 13-14 May period with transitions between dust intrusion, altitude depending mixing between dust and volcanic particles, a

completely volcanic phase and again the arrival of a large quantity of dust over a volcanic particles background.

At 04:00 UTC, on 13 May, dust and volcanic particles are simultaneously present but in well distinct layers located at different altitudes. Around 05:00 UTC, 13 May, a sort of interruption in this transport occurred with air masses coming from North Western Europe, very close to Iceland, where both satellite images and ground-based measurements show volcanic particle presence (Pappalardo et al., 2010a; Schumann et al., 2011). The analysis of multi-wavelength lidar measured permitted a detailed aerosol typing, distinguishing between volcanic layers (at upper levels) and mixing of dust and volcanic aerosol (at 05:00 UTC, between 3.2-6.4 km asl and at 06:00 UTC, between 3.4-4.3 km a.s.l.), mixing between dust and local aerosol (at 06:00 UTC below 3.4 km a.s.l.) and mixing between volcanic and local particles (starting from 07:00 UTC to 12:00 UTC, below 3-3.2 km a.s.l.). A mixing with PBL entrapped aerosol was observed until the evening. The long break in the aerosol mask in the early morning of 14 May is related to the presence of very low clouds and light rain. After this break, a mixing between Saharan dust and volcanic particles is observed in the 2-7 km a.s.l. altitude layer in the morning of the 14 May, when accordingly to DREAM and backtrajectories analysis dust contribution is not negligible and the transport of volcanic aerosol from Iceland was still continuing.

For the volcanic layer, a peak of $8x10^{-7}$ $m^{-1}sr^{-1}$ in the aerosol backscatter coefficient is observed. However, this period together with the peak of 20 April, 22:00 UTC correspond to the highest volcanic aerosol optical depth observed at CIAO with a value of 0.12 at 355 nm.

In terms of intensive properties, there is a significant difference **with respect** to the other cases. **Lidar ratio values are in between those observed in correspondence of the first arrival on 20 April and for after 21 April, while Ångström exponents are smaller than values typically observed in the previous days and a mean particle linear depolarization ratio of 16%, similar to 20 April case, is observed.**

4.1.4 18-19 May 2010

The last observation of volcanic particles over Potenza was recorded on 18-19 May between 2 and 5 km a.s.l., when there was no block of the air traffic over Italy or alert for volcanic particle arrival. During the same days, the reported mask identifies layers above 5 km a.s.l. whose origin cannot be clearly identified at this stage. For these days, backtrajectories do not clearly indicate the volcanic origin of the observed particles, but pass over continental Europe and the Atlantic Ocean. We could assume that these are volcanic particles because starting from the first explosive eruption on 15 April we have observed volcanic aerosol traces at these altitudes. However, as far as this case is concerned, the lack of multi-wavelength analyses due both to the sparse low clouds (about 60% of the time) and diurnal conditions does not permit a reliable typing of these layers.

4.2 Optical properties of volcanic aerosol

The dependence of intensive properties retrieved by lidar (backscatter-related Ångström exponent at 532/1064 nm, extinction and backscatter-related Ångström exponents at 355/532 nm, lidar ratio at 355 and 532 nm, and linear particle depolarization ratio) as a function of the relative humidity measured by the co-located microwave radiometer is investigated (Fig. 6). In particular, backscatter-related Ångström exponent at 532/1064 nm, å(β) (Fig.6a) and lidar ratio at 355 nm, S_{uv} (Fig. 6c) are preferred to Ångström exponent at 532/355 nm and lidar ratio at 532 nm, respectively, because of the larger availability of these data. The particle linear depolarization ratio, δ, is reported as a function of RH in Fig. 6b. In addition, the ratio of the lidar ratio at the 2 wavelengths, S_{uv}/S_{vis} is reported (Fig. 6d), since this parameter has been found to be important for the microphysical properties investigations (Muller et al. 2007).

The dependence on relative humidity of the backscatter-related Ångström exponent is the clear signature of the hygroscopic growth with the RH increase. A similar dependence on RH is found for the ratio of lidar ratios. The particle linear depolarization ratio shows **higher values in correspondence of higher RH**, that could indicate the presence of sulfate aerosols for the whole period (Sakai et al., 2000).

No clear RH dependence is found for S_{uv}: for the same RH value, low (around 40 sr) and high (around 85 sr) values are observed. In particular, low lidar ratio values are measured on 20 April. The S_{uv} value of 54 sr recorded for the same event on 19 April indicates an increase with RH for this specific event. The observations collected at CIAO from 19 to 20 April correspond both to the largest amount of transportable ash emitted by the volcano and the highest maximum emission height ranges (Matthias et al., 2011). On 13 May a similar situation is found in terms of transportable emitted aerosol and emission altitude. Indeed, these days are related to the strongest peaks, decreasing with the altitude, revealed in the temporal evolution of backscatter profiles. In addition, S_{uv} mean value measured in the volcanic layer on 13 May fits well with the S_{uv} dependence on RH observed for the 19-20 April data. This suggests differences in terms of the microphysical properties of volcanic particles reaching CIAO on 19-20 April and 13 May **with respect** to the other days.

A lidar ratio of about 40 sr at 355nm increasing with the relative humidity up to 60–70 sr, and a ratio of lidar ratios of about 0.8 was observed at CIAO on 19–20 April and 13 May 2010, dates corresponding to larger amount of aerosol emitted by the Icelandic volcano with respect to the other days under investigation. Lidar ratio values around 55 sr are reported in literature for fresh ash cases (Pappalardo et al., 2004a, Ansmann et al., 2010). This suggests the presence of some ash, besides sulfates, also in agreement with higher backscatter-related Ångström exponents for the same RH on these days **with respect** to all the other cases (see Fig. 6a). Moreover, there are some indications that the aging of aerosol through the European continent could affect the ratio of lidar ratios so as to lead this to values below 1 (Müller at al., 2007). In addition, the 19-20 April and 13 May cases correspond to the observation of ultra-giant particles signature in the cloud radar signals (Madonna et al., 2010b), furthermore confirming the different microphysical properties of the volcanic particles observed on these days.

For the other cases, 80 sr is obtained as lidar ratio in UV and the ratio of lidar ratios is greater than 1. This could be related to more mixing with continental and sulfates aerosol, in agreement with high S_{uv}, enlarged particles and the values of the ratio of lidar ratios (Ansmann et al., 2011; Muller et al., 2007).

At this stage the aerosol size distribution for the cases reported in Table 1 and Fig. 6 cannot be appropriately investigated on the basis of co-located AERONET measurements because only few AERONET data are available for the presence of clouds. Moreover, the Raman lidar (night-time) and AERONET (diurnal) measurements are not simultaneous, and the observed high variability in the aerosol content does not permit to use AERONET inversion for furthermore investigating the aerosol layers identified through the lidar measurements. A devoted study based both on the integration of lidar-radar measurements, with the support of all ancillary instrumentations available at CIAO, and a numerical simulation will be carried out in order to investigate the aerosol size and microphysical properties of these volcanic observations in depth.

5 Summary

The observations of Eyjafjallajökull volcanic cloud by multi-wavelength Raman lidar performed at CIAO observatory, in Southern Italy, are presented and discussed. **These measurements can be a reference point for the testing of atmospheric transport models. The observations are taken far from the source and the amount of volcanic aerosol reaching the measurement site is low.**

A methodology for the identification of the volcanic layer starting from temporal series of quality assured particle backscatter profiles is described **in detail**. With the support of model outputs, this methodology relies both on the multi-wavelength Raman lidar measurements and the long-term measurements performed at CIAO within EARLINET. The described methodology will be applied to all the EARLINET measurements performed during the Eyjafjallajökull eruption in 2010.

The aerosol masking for the 19 April – 20 May period shows that volcanic aerosol are observed at CIAO in 4 periods: 19-22 April, 27-29 April, 8-9 May, 13-14 May and 18-19 May. Volcanic layers are observed in the whole troposphere, with intrusions in the PBL on 21-22 April and 13 May. The co-presence of dust and volcanic aerosol is observed both at different levels and mixed with the same layer.

Two maxima of about 0.12-0.13 are found for volcanic layer aerosol optical depth at 355 nm on 20 April, 22:00 UTC and 13 May, 20:30 UTC. **These values are significantly lower than the peak values up to 0.7 at 532 nm observed over Germany in the volcanic layer during this event (Ansmann et al., 2010) and the moderate columnar AOD around 0.3-0.4 and 0.5 observed over Iberian peninsula (5-11 May) and Cabauw (17-21 May), respectively, for almost direct transport (Toledano et al., 2011; Ansmann et al., 2011). The low value observed at CIAO is related to the larger distance from the Eyjafjallajökull volcano and to the dispersion of the volcanic cloud during its path across Europe.**

A complete multi-wavelength analysis of the long-range transported volcanic aerosol is presented for the most significant time-windows. The dependence of lidar retrieved intensive properties on relative humidity is studied. **Typically high S_{uv}, particle linear depolarization ratio increasing with RH and values of the ratio of lidar ratios greater than 1 are measured in the volcanic aerosol layers at CIAO. These values suggest the presence of volcanic sulfates/continental mixed aerosol. Different intensive aerosol optical properties are measured at CIAO in correspondence of the maxima in the observed volcanic aerosol: lidar ratio increasing with RH (from 40 to 70 sr for RH from 20 to 70%) and**

ratio of lidar ratio values below 1. These values indicate the presence, besides sulfates aerosols, of some ash affected by the aging through the European continent. A devoted study based on the synergic use of all CIAO observatory instrumentations and in particular on lidar-radar integration will be carried out in order to investigate the aerosol size and microphysical properties for these volcanic observations in depth.

Acknowledgements

The financial support for EARLINET by the European Commission under grant RICA-025991 is gratefully acknowledged. We acknowledge the support of the European Commission through GEOmon Integrated Project under the 6th Framework Programme (contract number FP6-2005-Global-4-036677). The CIAO observatory is partially supported by the Italian Civil Protection Department of the Ministry Council.

Authors would like to thank the NOAA Air Resources Laboratory (ARL) for the provision of the HYSPLIT backtrajectory analysis; the German Weather Service for the air mass back-trajectory analysis, NILU for providing FLEXTRA back-trajectories based on meteorological data provided from ECMWF (European Centre for Medium Range Weather Forecast) and available at http://www.nilu.no/trajectories; and Tom L. Kucsera (GEST) at NASA/Goddard for back-trajectories available at the aeronet.gsfc.nasa.gov website. We also thank the Barcelona Supercomputing Center for forecasts with the Dust Regional Atmospheric Model (DREAM) and the Data User Element of the European Space Agency Data for data available from “ATSR World Fire Atlas”. The Eyjafjallajökull volcanic activity was monitored through updated reports provided by the Iceland Meteorological Office and available at http://en.vedur.is/earthquakes-and-volcanism/articles/nr/2072.

References

Ansmann, A., Riebesell, M., Wandinger U., Weitkamp C., Voss E., Lahmann W., and Michaelis W.: Combined Raman elastic-backscatter lidar for vertical profiling of moisture, aerosol extinction, backscatter and lidar ratio, Appl. Phys. B., 55, 18-28, 1992.

Ansmann, A., Tesche, M., Groß, S., Freudenthaler, V., Seifert, P., Hiebsch, A., Schmidt, J., Wandinger, U., Mattis, I., Müller, D., and Wiegner M.: The 16 April 2010 major volcanic ash plume over central Europe: EARLINET lidar and AERONET photometer observations at

Leipzig and Munich, Germany, Geophys. Res. Lett., 37, L13810, doi:10.1029/2010GL043809, 2010.

Ansmann, A., et al.: Ash and fine-mode particle mass profiles from EARLINET-AERONET observations over central Europe after the eruptions of the Eyjafjallajökull volcano in 2010, *J. Geophys. Res.*, 116, D00U02, doi:10.1029/2010JD015567, 2011.

Böckmann, C., Wandinger, U., Ansmann, A., Bösenberg, J., Amiridis, V., Boselli,A., Delaval, A., De Tomasi, F., Frioud, M., Grigorov, I., Hågård, A., Horvat, M., Iarlori,M., Komguem, L., Kreipl, S., Larchevêque, G., Matthias, V., Papayannis, A., Pappalardo, G., Rocadenbosch, F., Rodrigues, J.A., Schneider, J., Shcherbakov, V., and Wiegner M. al.:Aerosol lidar intercomparison in the framework of the EARLINET project. 2. Aerosol backscatter algorithms, Appl. Opt., 43, 977-989, 2004.

Di Girolamo, P., Ambrico, P. F., Amodeo, A., Boselli, A., Pappalardo, G., and Spinelli, N.: Aerosol observations by lidar in the nocturnal boundary layer, Appl. Opt., 38(21), 4585–4595, 1999.

Draxler, R.R. and Rolph, G.D.: HYSPLIT (HYbrid Single-Particle Lagrangian Integrated Trajectory) Model access via NOAA ARL READY Website (http://ready.arl.noaa.gov/HYSPLIT.php). NOAA Air Resources Laboratory, Silver Spring, MD, 2011.

Emeis, S., Forkel, R., Junkermann, W., Schäfer, K., Flentje, H., Gilge, S., Fricke, W., Wiegner, M., Freudenthaler, V., Groβ, S., Ries, L., Meinhardt, F., Birmili, W., Münkel, C., Obleitner, F., and Suppan, P.: Measurement and simulation of the 16/17 April 2010 Eyjafjallajökull volcanic ash layer dispersion in the northern Alpine region, Atmos. Chem. Phys., 11, 2689-2701, doi:10.5194/acp-11-2689-2011.

Flentje, H., Claude H., Elste T., Gilge S., Köhler U., Plass-Dülmer C., Steinbrecht W., Thomas W., Werner A., and Fricke W.: The Eyjafjallajökull eruption in April 2010 – detection of volcanic plume using in-situ measurements, ozone sondes and a new generation ceilometer network Atmos. Chem. Phys. Discuss., 10, 14947-14968, 2010.

Freudenthaler, V., Esselborn, M., Wiegner, M., Heese, B., Tesxhe, M., Ansmann, A., Müller, D., Althausen, D., Wirth, M., Fix, A., Ehret, G., Knippertz, P., Toledano, C., Gasteiger, J., Garhammer, M. and Seefeldner, M. : Depolarization ratio profiling at several wavelengths in pure Saharan dust during SAMUM 2006. Tellus B, 61: 165–179. doi: 10.1111/j.1600-0889.2008.00396, 2009.

Gasteiger, J., Groß S., Freudenthaler V., and Wiegner M.: Volcanic ash from Iceland over Munich: mass concentration retrieved from ground-based remote sensing measurements, Atmos. Chem. Phys., 11, 2209-2223, 2011.

Langmann, B., Folch, A., Hensch, M., Matthias, V.: Volcanic ash over Europe during the eruption of Eyjafjallajökull on Iceland, April-May 2010, in press on Atmospheric Environment, 2011.

Lettino A., Caggiano R., Fiore S., Macchiato M., Sabia S., Trippetta S.: Eyjafjallajökull volcanic ash in southern Italy. Atm. Env., doi: 10.1016/j.atmosenv.2011.05.037, 2011.

Liu, Z., R. Kuehn, M. Vaughan, D. Winker, A. Omar, K. Powell, C. Trepte, Y. Hu, and C. Hosttler: The CALIPSO cloud and aerosol discrimination: version 3 algorithm and test results - Proceedings of the 25th International Laser Radar Conference, 1245–1248, St. Petersburg, Russia, 5–9 July 2010, 2010.

Madonna, F., Amodeo, A., Boselli, A., Cornacchia, C., D'Amico, G., Giunta, A., Mona, L., Pappalardo, G., and Cuomo, V. : CIAO: the CNR-IMAA advanced observatory for atmospheric research, Atmos. Meas. Tech. Discuss., 3, 5253-5293, doi:10.5194/amtd-3-5253-2010, 2010a.

Madonna, F., Amodeo A., D'Amico G., Mona L., and Pappalardo G.: Observation of non-spherical ultragiant aerosol using a microwave radar, Geophys. Res. Lett., 37, L21814, doi:10.1029/2010GL044999, 2010b.

Matthias, V., Balis, D., Bösenberg, J., Eixmann R., Iarlori M., Komguem L., Mattis I., Papayannis A., Pappalardo G., Perrone M.R. and Wang X. et al.: The vertical aerosol distribution over Europe: statistical analysis of Raman lidar data from 10 EARLINET stations, J. Geophys. Res., 109, D18201, doi:10.1029/2004JD004638, 2004.

Matthias,V., Aulingera A., Biesera J., Cuesta J., Geyera B., Langmanne B., Serikov I., Mattis I., Minikin A., Mona L., Quante M., Schumann U., Weinzierl B.: The ash dispersion over Europe during the Eyjafjallajökull eruption - comparison of CMAQ simulations to remote sensing and in-situ observations, submitted to Atmospheric Environment, 2011.

Mona, L., Amodeo A., D'Amico G., Pandolfi M., Pappalardo G.: Lidar ratio climatology: 5 years of systematic Raman lidar measurements over Potenza, Italy – 23rd International Laser Radar Conference, Nara Japan, 24-28 July 2006, vol. 1, 321-324, 2006a.

Mona, L., Amodeo A., Pandolfi M., and Pappalardo G.: Saharan dust intrusions in the Mediterranean area: Three years of Raman lidar measurements, J. Geophys. Res., 111, D16203, doi:10.1029/2005JD006569, 2006b.

Mona, L., Cornacchia C., D'Amico G., Di Girolamo P., Pappalardo G., Pisani G., Summa D., Wang X., Cuomo V.: Characterization of the variability of the humidity and cloud fields as observed from a cluster of ground-based lidar systems, Q. J. R. Meteorol. Soc. 133: (S3) 257–271, 2007.

Mona, L., Pappalardo, G., Amodeo, A., D'Amico, G., Madonna, F., Boselli, A., Giunta, A., Russo, F., and Cuomo, V.: One year of CNR-IMAA multi-wavelength Raman lidar measurements in coincidence with CALIPSO overpasses: Level 1 products comparison, Atmos. Chem. Phys., 9, 7213-7228, doi:10.5194/acp-9-7213-2009, 2009

Morille Y., Haeffelin M., Drobinski P., Pelon J.: STRAT: An Automated Algorithm to Retrieve the Vertical Structure of the Atmosphere from Single-Channel Lidar Data, Jour. Atm. Ocean. Tech, 24, 761-775, 2007.

Müller, D., Ansmann A., Mattis I., Tesche M., Wandinger U., Althausen D., and Pisani G.: Aerosol-type-dependent lidar ratio observed with Raman lidar. J. Geophys. Res., 112, 2006JD008292, 2007.

Müller, D., Heinold B., Tesche M., Tegen I., Althausen D., Alados Arboledas L., Amiridis V., Amodeo A., Ansmann A., Balis D., Comeron A., D'Amico G., Gerasopoulos E., Guerrero-Rascado J. L., Freudenthaler V., Giannakaki E., Heese B., Iarlori M., Knippertz P., Mamouri R. E., Mona L., Papayannis A., Pappalardo G., Perrone R.-M., Pisani G., Rizi V., Sicard M., Spinelli N., Tafuro A., and Wiegner M.: EARLINET observations of the 14- 22-May long-range dust transport event during SAMUM 2006: validation of results from dust transport modelling. Tellus, 61B, 325-339, 2009.

Papayannis, A., Amiridis V., Mona L., Tsaknakis G., Balis , Bösenberg J., Chaikovski A., De Tomasi F., Grigorov I., Mattis I., Mitev V., Müller D., Nickovic S., Pérez C., Pietruczuk A., Pisani G., Ravetta F., Rizi V., Sicard M., Trickl T., Wiegner M., Gerding M., D'Amico G. and Pappalardo G.: Systematic lidar observations of aerosol optical properties during Saharan dust intrusions over Europe, in the frame of EARLINET (2000-2002): Statistical analysis and results, J. Geophys. Res., 113, D10204, doi:10.10129/2007JD9028, 2008.

Pappalardo G., A. Amodeo, L. Mona, M. Pandolfi, N. Pergola, V. Cuomo: Raman lidar observations of aerosol emitted during the 2002 Etna eruption, Geophys. Res. Lett., 31, L05120, doi:10.1029/2003GL019073, 2004a.

Pappalardo, G., Amodeo A., Pandolfi M., Wandinger U., Ansmann A., Bosenberg J., Matthias V., Amiridis V., De Tomasi F., Frioud M., Iarlori M., Komguem L., Papayannis A., Rocadenbosch F., Wang X.: Aerosol lidar intercomparison in the framework of the EARLINET project. 3. Raman lidar algorithm for aerosol extinction, backscatter and lidar ratio, Appl. Opt.,43, 5370-5385, 2004b.

Pappalardo, G., Amodeo A.; Ansmann A.; Apituley A.; Alados Arboledas L.; Balis D.; Böckmann C.; Chaikovsky A.; Comeron A.; D'Amico G.; De Tomasi F.; Freudenthaler V.; Giannakaki E.; Giunta A.; Grigorov I.; Gustafsson O.; Gross S.; Haeffelin M.; Iarlori M.; Kinne S.; Linné H.; Madonna F.; Mamouri R.; Mattis I.; McAuliffe M.; Molero F.; Mona L.;

Müller D.; Mitev V.; Nicolae D.; Papayannis A.; Perrone M. R.; Pietruczuk A.; Pujadas M.; Putaud J.-P.; Ravetta F.; Rizi V.; Serikov I.; Sicard M.; Simeonov V.; Spinelli N.; Stebel K.; Trickl T.; Wandinger U.; Wang X.; Wagner F.; Wiegner M.: EARLINET observations of the Eyjafjallajökull ash plume over Europe, in "Lidar Technologies, Techniques, and Measurements for Atmospheric Remote Sensing VI", Proceedings of SPIE, SPIE Remote Sensing 2010, Toulouse, 20 - 23 September 2010, vol: 7832, pp. 78320, 2010a.

Pappalardo G., Amodeo A.; Ansmann A.; Apituley A.; Alados Arboledas L.; Balis D.; Böckmann C.; Chaikovsky A.; Comeron A.; D'Amico G.; De Tomasi F.; Freudenthaler V.; Giannakaki E.; Giunta A.; Grigorov I.; Gustafsson O.; Gross S.; Haeffelin M.; Iarlori M.; Kinne S.; Linné H.; Madonna F.; Mamouri R.; Mattis I.; McAuliffe M.; Molero F.; Mona L.; Müller D.; Mitev V.; Nicolae D.; Papayannis A.; Perrone M. R.; Pietruczuk A.; Pujadas M.; Putaud J.-P.; Ravetta F.; Rizi V.; Serikov I.; Sicard M.; Simeonov V.; Spinelli N.; Stebel K.; Trickl T.; Wandinger U.; Wang X.; Wagner F.; Wiegner M.: Dispersion and evolution of the Eyjafjallajökull ash plume over Europe: vertically resolved measurements with the European LIDAR network EARLINET, 7th European Geosciences Union (EGU) General Assembly 2010, Vienna, Austria, 02–07 May 2010, EGU2010-15731, 2010b.

Pappalardo, G., Wandinger U., Mona L., Hiebsch, A., Mattis, I., Amodeo, A., Ansmann, A., Seifert, P., Linné, H., Apituley, A., Alados Arboledas, L., Balis, D., Chaikovsky, A., D'Amico, G., De Tomasi, F., Freudenthaler, V., Giannakaki, E., Giunta, A., Grigorov, I., Iarlori, M., Madonna, F., Mamouri, R.-E., Nasti, L., Papayannis, A., Pietruczuk, A., Pujadas, M., Rizi, V., Rocadenbosch, F., Russo, F., Schnell, F., Spinelli, N., Wang, X., Wiegner, M.: EARLINET correlative measurements for CALIPSO: First intercomparison results, J. Geophys. Res., 115, D00H19, doi:10.1029/2009JD012147, 2010c.

Petersen, G. N.: A short meteorological overview of the Eyjafjallajökull eruption 14 April–23 May 2010. Weather, 65: 203–207. doi: 10.1002/wea.634, 2010.

Sakai, T., Shibata T., Kwon S., Kim Y., Tamura K., Iwasaka Y.: Free tropospheric aerosol backscatter, depolarization ratio, and relative humidity measured with the Raman lidar at Nagoya in 1994-1997: contributions of aerosols from the Asian Continent and the Pacific Ocean, Atmospehric Environmet, 34, 431-442, 2000.

Schoeberl, M. R., and Newman P. A.: A multiple-level trajectory analysis of vortex filaments, J. Geophys. Res., 100, 25,801-25,816, 1995.

Schumann, U., Weinzierl, B., Reitebuch, O., Schlager, H., Minikin, A., Forster, C., Baumann, R., Sailer, T., Graf, K., Mannstein, H., Voigt, C., Rahm, S., Simmet, R., Scheibe, M., Lichtenstern, M., Stock, P., Rüba, H., Schäuble, D., Tafferner, A., Rautenhaus, M., Gerz, T., Ziereis, H., Krautstrunk, M., Mallaun, C., Gayet, J.-F., Lieke, K., Kandler, K., Ebert, M., Weinbruch, S., Stohl, A., Gasteiger, J., Groß, S., Freudenthaler, V., Wiegner, M., Ansmann, A., Tesche, M., Olafsson, H., and Sturm, K.: Airborne observations of the Eyjafjalla volcano ash cloud over Europe during air space closure in April and May 2010, Atmos. Chem. Phys., 11, 2245-2279, doi:10.5194/acp-11-2245-2011, 2011.

Steyn, D., Baldi G. M., Hoff R. M.: The Detection of Mixed Layer Depth and Entrainment Zone Thickness from Lidar Backscatter Profiles, Journal of Atmospheric and Oceanic Technology, 16, 7, 953-959, doi: 10.1175/1520-0426(1999)016, 1999.

Stohl, A., Wotawa G., Seibert P., and Kromp-Kolb H.: Interpolation errors in wind fields as a function of spatial and temporal resolution and their impact on different types of kinematic trajectories. J. Appl. Meteor. 34, 2149-2165, 1995.

Stohl, A.: Computation, accuracy and applications of trajectories - a review and bibliography. Atmos. Environ. 32, 947-966, 1998.

Stohl, A., Prata A. J., Eckhardt S., Clarisse L., Durant A., Henne S., Kristiansen N. I., Minikin A., Schumann U., Seibert P., Stebel K., Thomas H. E., Thorsteinsson T., Tørseth K., and Weinzierl B.: Determination of time- and height-resolved volcanic ash emissions for quantitative ash dispersion modeling: the 2010 Eyjafjallajökull eruption, Atmos. Chem. Phys. Discuss., 11, 5541-5588, 2011.

Toledano C. et al.: Aerosol, properties derived from Sun photometer and satellite observations of the Eyjafjallajökull ashes over the Iberian Peninsula, Atmospheric Environment, in press, 2011.

Vaughan M., Young S., Winker D., Powell K., Omar A., Liu Z., Hu Y., Hostetler C.: Fully automated analysis of space-based lidar data: an overview of the CALIPSO retrieval algorithms and data products, in “Laser Radar Techniques for Atmospheric Sensing”, Proceedings of SPIE, SPIE 2004, Bellingham, WA, USA, Vol. 5575, doi: 10.1117/12.572024, 2004.

Villani, M. G., Mona L., Maurizi A., Pappalardo G., Tiesi A., Pandolfi M., D’Isidoro M., Cuomo V., and Tampieri F. : Transport of volcanic aerosol in the troposphere: the case study of the 2002 Etna plume, J. Geophys. Res., 111, doi:10.1029/2006JD007126, 2006.

Wang, L., Sassen K.: Wavelet Analysis of Cirrus Multiscale Structures from Lidar Backscattering: A Cirrus Uncinus Complex Case Study, Journal of Applied Meteorology and Climatology, 47, 10, 2645-2658, doi: 10.1175/2008JAMC1788.1, 2008.

Table 1. Intensive properties calculated within identified volcanic layers. Mean values and standard deviations of the lidar ratio at 355nm (S_{uv}) and 532 nm (S_{vis}); Ångström exponent at 355/532 nm (å(α)); backscatter related Ångström exponent at 532/1064 nm (å(β)) and particle linear depolarization ratio at 532 nm (δ) are reported.

Time (UTC)	**Altitude [km a.s.l.]**	**S_{uv} [sr]**	**S_{vis} [sr]**	**å(α)**	**å(β)**	**δ**
19:53-20:24 19April	2.1 -4.2	54 ± 14	n.a.	n.a.	n.a.	n.a.
21:00-23:05 20 April	2-3	42 ± 2	50 ± 3	1.4 ± 0.2	1.8 ± 0.1	0.15 ± 0.03
	3.1-4	38 ± 6	n.a.	n.a.	1.8 ± 0.1	0.22 ± 0.03
11:30-12:30 21 April	1.6 - 3.6	n.a.	n.a.	n.a.	1.3 ± 0.7	n.a.
19:07-03:09 21-22 April	1.6-3.4	80 ± 12	78 ± 13	1.1 ± 0.3	1.21 ± 0.07	0.25 ± 0.05
22:17-23:24 29 April	2.7-3.4	80 ± 17	92 ± 16	1.4 ± 0.3	1.39 ± 0.04	n.a.
19:03-21:58 09 May	1.6-2.5	89 ± 11	78 ± 15	1.03 ± 0.07	1.5 ± 0.6	0.14 ± 0.04
	2.5-5	n.a.	n.a.	n.a.	2.1 ± 0.5	0.10 ± 0.09
20:16-21:01 13 May	1.5-2.3	60 ± 11	78 ± 12	1.1 ± 0.4	0.82 ± 0.03	0.16 ± 0.07
	2.3-2.6	60 ± 7	n.a.	n.a.	1.04 ± 0.07	n.a.

Figure 1. Temporal evolution of range corrected lidar signal measured at 1064 nm in the 12-14 May period by PEARL at CIAO. The vertical and temporal resolutions are respectively 7.5 m and 30 s.

Figure 2. Example of single profile particle layer identification as performed on the aerosol backscatter profile at 1064 nm measured on 13 May, at 05:30-06:30 UTC. Horizontal dotted and solid lines indicate the base and top of the identified layers, respectively. Red square indicates the PBL top height. Region with relative errors between 30 and 50% are reported in blue and those with relative error exceeding 50% in green.

Figure **3.** Profiles of the aerosol backscatter at 1064 nm and of the backscatter related Ångström exponent at 532/1064 nm measured on 13 May, at 04:00, 05:00 and 06:00 UTC. **Mean values are reported as squares for backscatter related Ångström exponent at altitude levels where statistical errors are larger than 30%.** Error bars report the standard errors for the mean values.

Figure **4**. Aerosol masks related to 19-22 April, 27-29 April and 08-10 May 2010 periods are reported in chronological order from the top to the bottom.

Figure **5**. Aerosol masks related to 13-14 May and 18-19 May 2010 periods are reported in chronological order from the top to the bottom.

Figure 6. Intensive properties calculated with identified volcanic layers are reported as a function of the relative humidity as measured by the co-located microwave profiler. The backscatter related Ångström exponent at 532/1064 nm (å(β)), the lidar ratio at 355 nm (S_{uv}), the ratio of lidar ratios (S_{uv}/S_{vis}), and the particle linear depolarization ratio at 532nm (δ) are reported respectively in panels a, b, c and d. Standard deviations are reported as error bars.

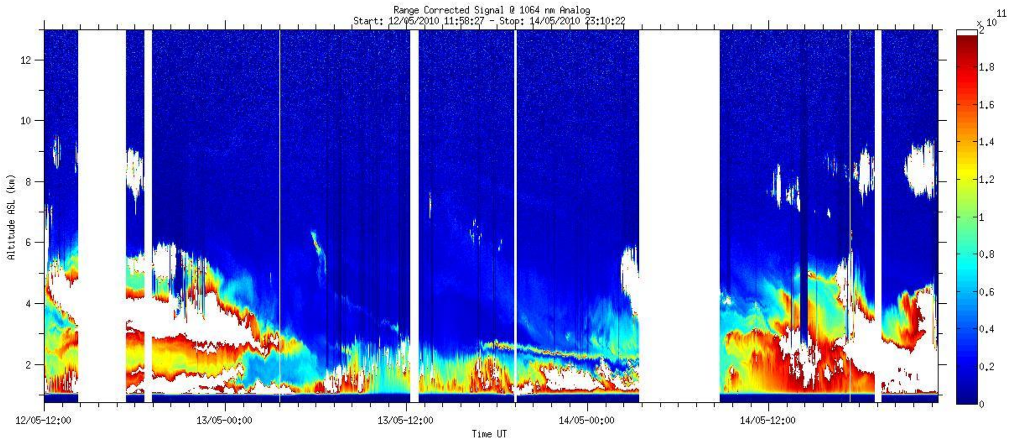

Figure 1. Temporal evolution of range corrected lidar signal measured at 1064 nm in the 12-14 May period by PEARL at CIAO. The vertical and temporal resolutions are respectively 7.5 m and 30 s.

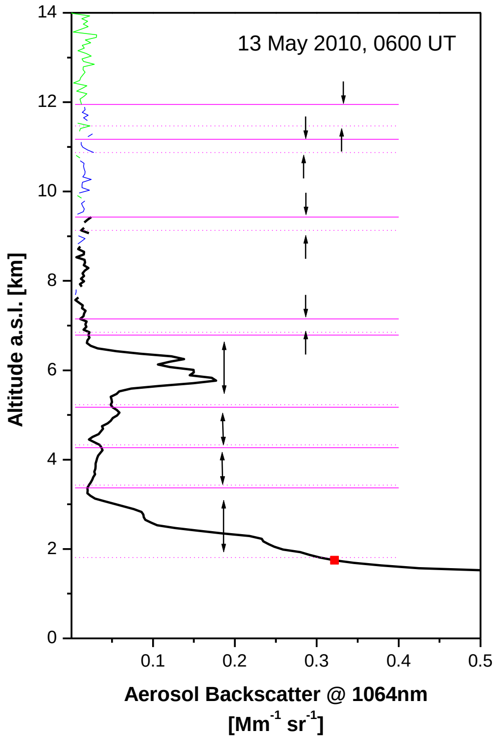

Figure 2. Example of single profile particle layer identification as performed on the aerosol backscatter profile at 1064 nm measured on 13 May, at 05:30-06:30 UTC. Horizontal dotted and solid lines indicate the base and top of the identified layers, respectively. Red square indicates the PBL top height. Region with relative errors between 30 and 50% are reported in blue and those with relative error exceeding 50% in green.

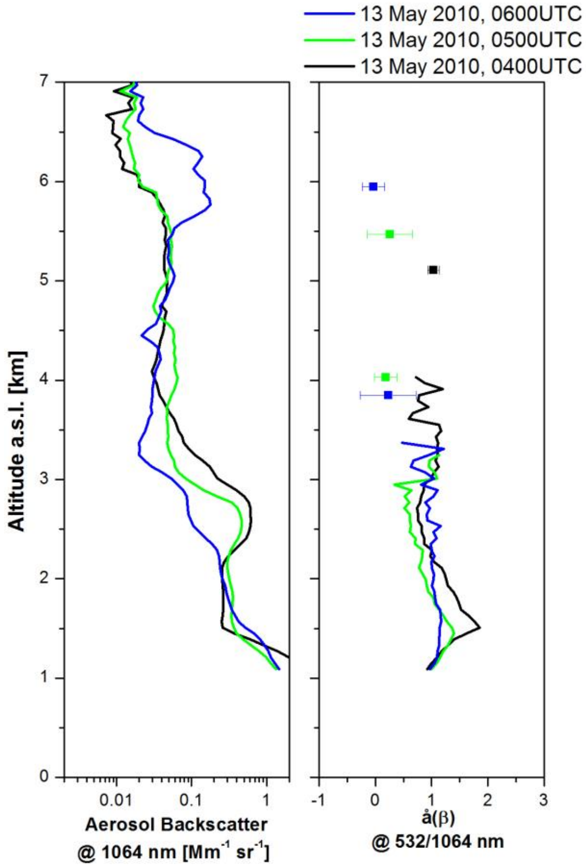

Figure **3.** Profiles of the aerosol backscatter at 1064 nm and of the backscatter related Ångström exponent at 532/1064 nm measured on 13 May, at 04:00, 05:00 and 06:00 UTC. **Mean values are reported as squares for backscatter related Ångström exponent at altitude levels where statistical errors are larger than 30%.** Error bars report the standard errors for the mean values.

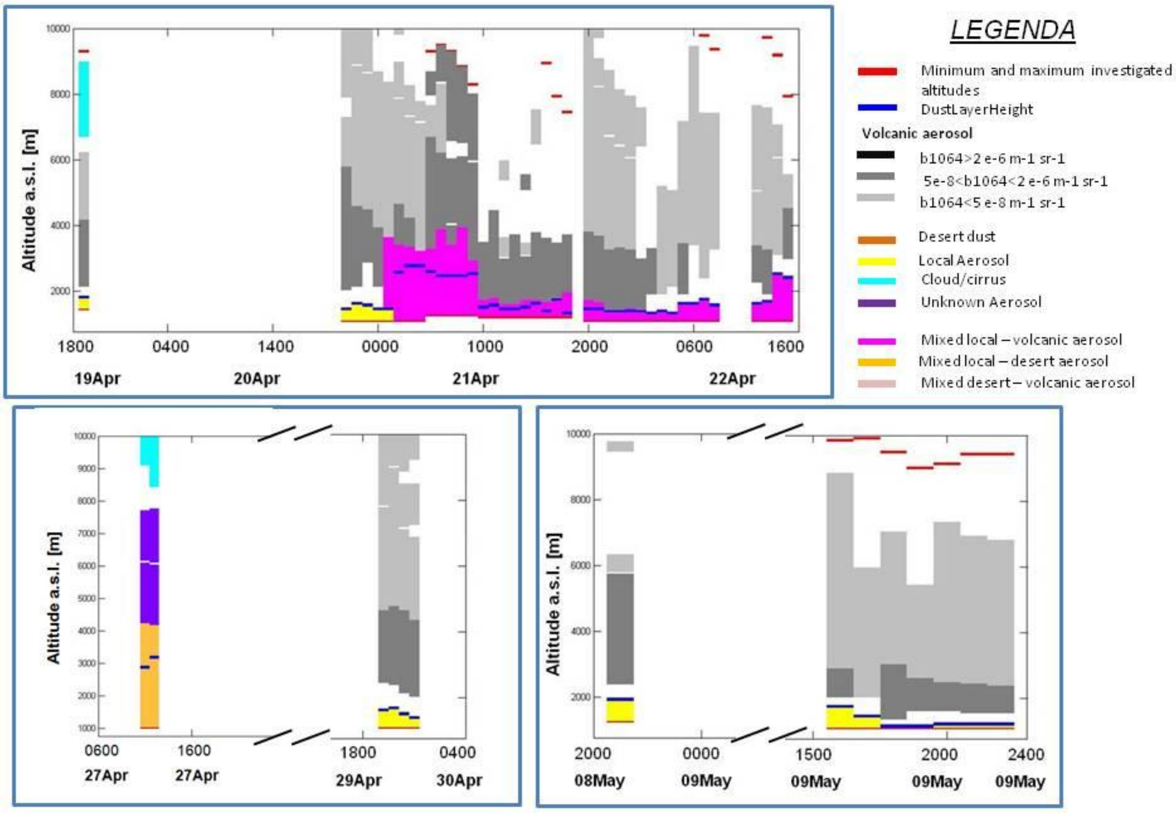

Figure **4**. Aerosol masks related to 19-22 April, 27-29 April and 08-10 May 2010 periods are reported in chronological order from the top to the bottom.

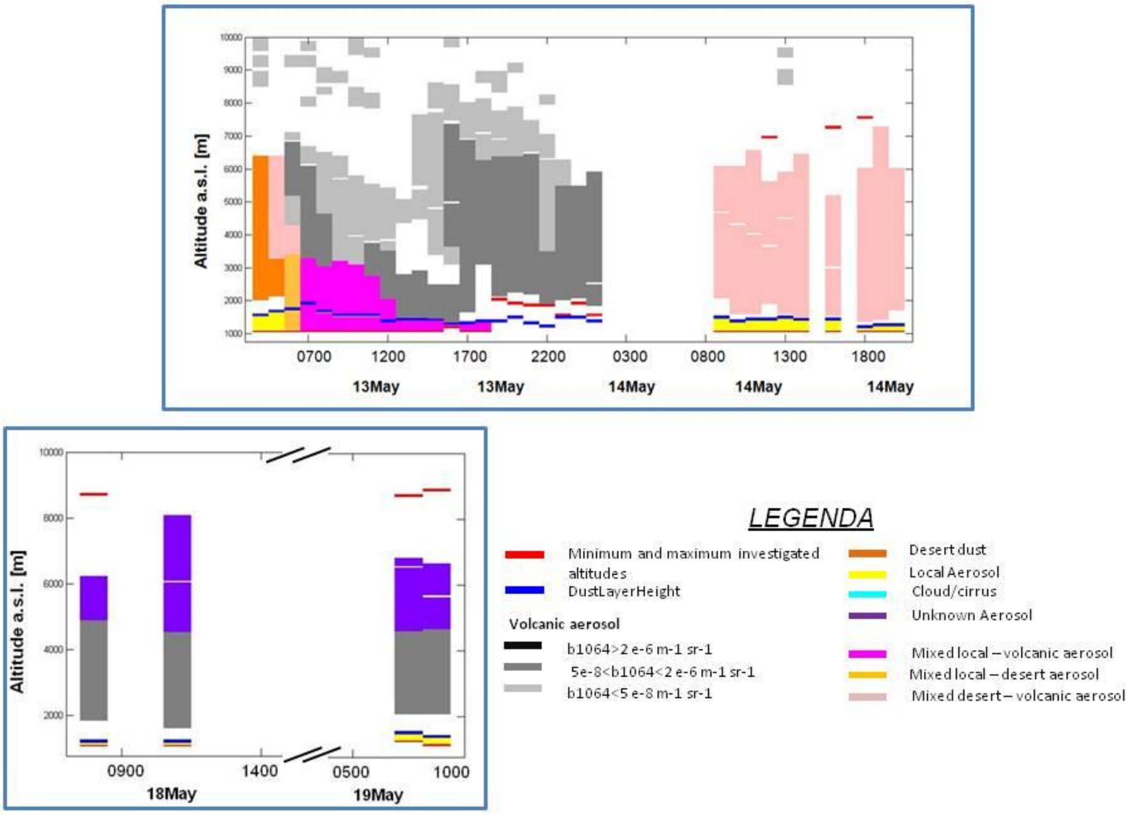

Figure **5**. Aerosol masks related to 13-14 May and 18-19 May 2010 periods are reported in chronological order from the top to the bottom.

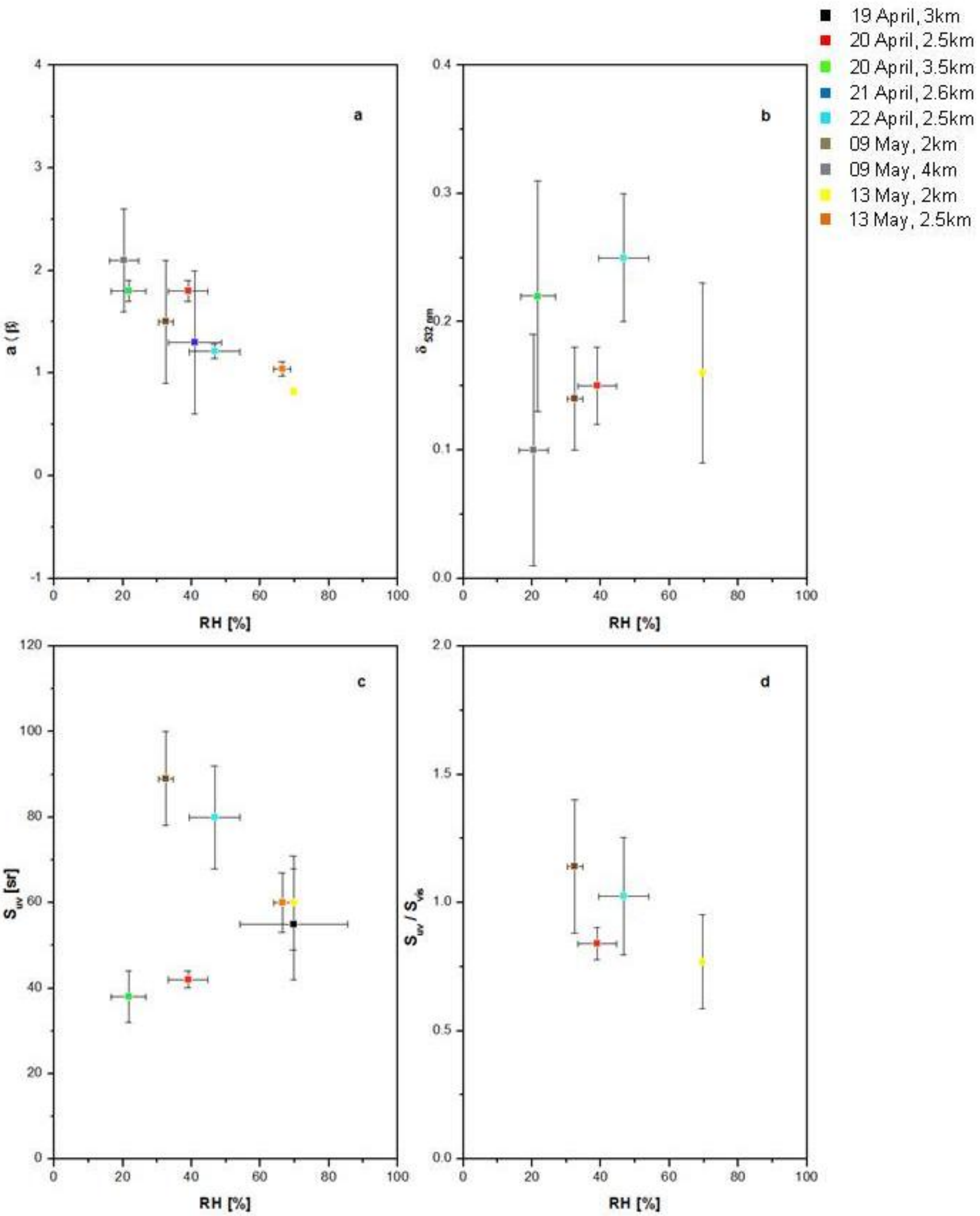

Figure 6. Intensive properties calculated with identified volcanic layers are reported as a function of the relative humidity as measured by the co-located microwave profiler. The backscatter related Ångström exponent at 532/1064 nm (å(β)), the lidar ratio at 355 nm (S_{uv}), the ratio of lidar ratios (S_{uv}/S_{vis}), and the particle linear depolarization ratio at 532nm (δ) are reported respectively in panels a, b, c and d. Standard deviations are reported as error bars.